



## Revealing a role for the G subunit in mediating interactions between the nitrogenase component proteins

Natasha Pence<sup>a,b</sup>, Nathan Lewis<sup>a,1</sup>, Alexander B. Alleman<sup>a</sup>, Lance C. Seefeldt<sup>c</sup>, John W. Peters<sup>a,\*</sup>

<sup>a</sup> Institute of Biological Chemistry, Washington State University, Pullman, WA 99164, United States of America

<sup>b</sup> Department of Chemistry and Biochemistry, Montana State University, Bozeman, MT 59717, United States of America

<sup>c</sup> Department of Chemistry and Biochemistry, Utah State University, Logan, UT 84322, United States of America



### ARTICLE INFO

#### Keywords:

Electron transfer  
Homology modeling  
Transcriptomics  
Differential gene expression  
Protein-protein interaction  
Nitrogenase

### ABSTRACT

*Azotobacter vinelandii* contains three forms of nitrogenase known as the Mo-, V-, and Fe-nitrogenases. They are all two-component enzyme systems, where the catalytic component, referred to as NifDK, VnfDGK, and AnfDGK, associates with the reductase component, the Fe protein or NifH, VnfH, and AnfH respectively. AnfDGK and VnfDGK have an additional subunit compared to NifDK, termed gamma or AnfG and VnfG, whose role is unknown. The expression of each nitrogenase is tightly regulated by metal availability, however it is known that there is crosstalk between the Mo- and V-nitrogenases but the Fe-nitrogenase components cannot support substrate reduction with its Mo-nitrogenase counterparts. Here, docking models for the nitrogenase complexes were generated in ClusPro 2.0 based on the crystal structure of the Mo-nitrogenase and refined using the HADDOCK 2.2 refinement interface to identify structural determinants that enable crosstalk between the Mo- and V-nitrogenase but not the Fe-nitrogenase. Differing salt bridge interactions were identified at the binding interface of each complex. Specifically, positively charged residues of VnfG enable complementary interactions with NifH and VnfH but not AnfH. Similarly, negatively charged residues of AnfG enable interactions with AnfH but not NifH or VnfH. A role for the G subunit is revealed where VnfG could be mediating crosstalk between the Mo- and V-nitrogenases while the AnfG subunit on AnfDGK makes interactions with NifH and VnfH unfavorable, reducing competition with NifDK and funneling electrons to the most efficient nitrogenase.

### 1. Introduction

The most efficient and well-studied nitrogenase in *A. vinelandii* is the molybdenum-dependent nitrogenase or Mo-nitrogenase [1–3]. The Mo-nitrogenase is made up of two component proteins, the catalytic component known as the MoFe protein (NifDK) and the Fe protein (NifH) that functions in electron delivery [4,5]. NifDK has two unique metallocofactors: the P-cluster, which delivers electrons to the FeMo-cofactor, the site for substrate reduction [6,7]. NifH is a homodimer with a single bridging [4Fe-4S] cluster involved in electron delivery to NifDK [8]. NifH transiently associates with NifDK through a process known as the Fe protein cycle [4,9]. NifH is reduced by a low potential electron carrier such as flavodoxin or ferredoxin, followed by nucleotide exchange for ATP [9,10]. This nucleotide exchange induces

conformational changes that enable NifH to bind and transfer an electron to NifDK where subsequent ATP hydrolysis, release of P<sub>i</sub>, and complex dissociation occurs [11–15]. The overall process requires 16 ATP and 8 low potential electrons to fully reduce dinitrogen to two molecules of ammonia with concomitant production of H<sub>2</sub> under optimal *in vitro* conditions [16,17].

The alternative nitrogenases, known as the V- and Fe-nitrogenases, are also two-component enzyme systems where the catalytic component is known as the VFe (VnfDGK), and FeFe (AnfDGK) proteins and the component involved in electron delivery is the Fe protein designated VnfH and AnfH [1,3,18,19]. The alternative nitrogenases have analogous metallocofactors to NifDK except for the identity of the heteroatom (V or Fe) at their active sites and the FeV-cofactor has carbonate which replaces a bridging sulfur, but it is not known if the FeFe-cofactor has

**Abbreviations:** NifDK, MoFe protein; VnfDGK, VFe protein; AnfDGK, FeFe protein; DGE, differential gene expression.

\* Corresponding author.

E-mail address: [jw.peters@wsu.edu](mailto:jw.peters@wsu.edu) (J.W. Peters).

<sup>1</sup> Present address: Department of Plant and Microbial Biology University of Minnesota, Minneapolis MN 55108

<https://doi.org/10.1016/j.jinorgbio.2020.111273>

Received 1 June 2020; Received in revised form 16 September 2020; Accepted 3 October 2020

Available online 7 October 2020

0162-0134/© 2020 Elsevier Inc. All rights reserved.

carbonate or sulfide at that specific belt position [20]. They also have additional subunits designated VnfG or AnfG. The exact role of this additional subunit is unknown however they are required for Mo-independent diazotrophic growth [20,21]. The G subunit does influence substrate specificity, as strains with mutations in *anfG* and *vnfG* were able to reduce acetylene but not N<sub>2</sub> [21]. The G subunit has also been proposed to be involved in FeV-cofactor delivery, which is supported by the crystal structure of VnfdGK where VnfG is located near the cofactor insertion site but away from the P-cluster [20,22].

The alternative nitrogenases are less efficient at N<sub>2</sub> reduction and require 24 ATP and 12 low potential electrons for the V-nitrogenase and 40 ATP and 20 low potential electrons for the Fe-nitrogenase to reduce 1 mol of N<sub>2</sub> [16,23,24]. They also have different limiting stoichiometries for H<sub>2</sub> produced per N<sub>2</sub> reduced: 1:1 for the Mo-nitrogenase, 3:1 for the V-nitrogenase, and 7:1 for the Fe-nitrogenase [16,19,24]. This has been hypothesized to be potentially attributed to differences in the reactivity for N<sub>2</sub> binding at the active site where Mo > V > Fe [16].

The Mo-, V-, and Fe-nitrogenases are mechanistically similar but genetically distinct as they are encoded in separate gene clusters designated *nif*, *vnf*, and *anf* [16,25,26]. The expression of all three nitrogenase homologs are tightly regulated by metal availability in the environment [3,25,27–29]. The *nif* genes are always preferentially expressed when Mo is present. In the absence of Mo and presence of V, genes in the *vnf* gene cluster are expressed, and in the absence of Mo and V, genes in the *anf* gene cluster are expressed [25].

Due to the high metabolic cost required to meet the demand to fix N<sub>2</sub> and the presence of *A. vinelandii* in diverse soil environments, the alternative nitrogenases are thought to expand the niche for diazotrophy in response to differing metal availability [25,30]. Therefore, it is reasonable to consider situations where *A. vinelandii* would have to finely tune expression of all three nitrogenases to accomplish efficient biological nitrogen fixation where Mo is limited.

Indeed, it is known that the V-nitrogenase components can support catalysis with their Mo-nitrogenase counterparts [31,32]. *A. vinelandii* NifDK was reported to have a higher specific activity for acetylene reduction when complemented with VnfH compared to NifH [31]. *A. vinelandii* VnfdGK complemented with NifH had approximately 63% specific activity for acetylene reduction compared to NifDK/NifH [31]. The Fe-nitrogenase components however show markedly reduced activities when complemented with their Mo-nitrogenase counterparts [19]. Acetylene reduction by NifDK complemented with AnfH from *R. capsulatus* was reported to have 10–15% of the specific activity compared to NifDK/NifH [19]. Additionally, acetylene reduction by AnfDGK complemented with NifH from *R. capsulatus* had very low specific activity of 1–2% compared to AnfDGK/AnfH [19]. It is unknown if the V-nitrogenase components can support catalysis when mixed with their Fe-nitrogenase counterparts.

The three nitrogenase systems in *A. vinelandii* have been characterized to varying degrees, and structural information on the Fe- and V-nitrogenases is incomplete. The Mo-nitrogenase complex is currently the only nitrogenase system with complete structural data [6,8,33–35]. Recently, structures of VnfdGK and the ADP-bound state of VnfH were published providing important structural information about the location of the G subunit on VnfdGK [20,36]. To date, the Fe-nitrogenase remains structurally uncharacterized. Therefore, a homology modeling approach was used here to fill these gaps in structural information, allowing for comparison of the structural determinants for cross-reactions between the Mo-nitrogenase and V-nitrogenase components that deter reactions with the Fe-nitrogenase.

Structural differences between the nitrogenases were examined, and properties were observed that could functionally differentiate them by comparing the interactions mediated by the G subunit of VnfdGK and AnfDGK with VnfH, AnfH and NifH. Our results suggest a structural mechanism to direct electron flow to the most efficient Mo-nitrogenase, where the likelihood of productive electron transfer associations are increased.

**Table 1**  
Template and PDB information for the homology modeling.

Protein	Template	PDB entry	Template source
VnfH	<i>A. vinelandii</i> MgAMPPCP-bound	4WZB	Tezcan et al., 2005 [35]
ATP	NifH		
AnfH	<i>A. vinelandii</i> MgAMPPCP-bound	4WZB	Tezcan et al., 2005 [35]
ATP	NifH		
AnfD	<i>A. vinelandii</i> VnfD	5N6Y	Sippel et al., 2017 [20]
AnfG	<i>A. vinelandii</i> VnfG	5N6Y	Sippel et al., 2017 [20]
AnfK	<i>A. vinelandii</i> VnfK	5N6Y	Sippel et al., 2017 [20]

## 2. Materials and methods

### 2.1. Transcriptomic analysis under different metal-dependent diazotrophic conditions

RNA-seq data from a previous study of *A. vinelandii* under four growth conditions: 1) Ammonia (Non-diazotrophic or BN) 2) Mo-dependent (*nif* conditions) 3) V-dependent (*vnf* conditions), 4) Fe-dependent (*anf* conditions) was used for the differential gene expression analysis [25]. Data were published as the log<sub>2</sub> fold change in gene expression between non-diazotrophic and the different metal-dependent diazotrophic conditions. These values were then compared between the different metal-dependent conditions to calculate the DGE. The expression of candidate nitrogenase structural and electron transfer genes associated with Mo, V-, and Fe-dependent diazotrophy were then compared with a heatmap created in R 3.4 using the heatmap2 package [37].

### 2.2. Homology modeling of the ATP-bound state of the Fe proteins and the Fe-nitrogenase components

Homology models were built for the Fe-nitrogenase components (AnfDGK and AnfH). SWISS-MODEL was used to generate the individual subunits (AnfD, AnfG, and AnfK) using their V-nitrogenase counterparts as templates (Table 1) (PDB entry 5N6Y) [38]. The subunits were then docked in ClusPro 2.0 and aligned to the structure of VnfdGK (PDB entry 5N6Y) [39].

The subunits of VnfH and AnfH were modeled independently to represent the proposed conformational changes involved with the binding of MgATP based on the structure of the NifH bound to the non-hydrolysable ATP analog, MgAMPPCP (PDB entry 4WZB). The subunits were then docked in ClusPro 2.0 and aligned to the MgAMPPCP-bound NifH structure (PDB entry 4WZB) [39]. Table 1 shows the template information used for the homology modeling.

### 2.3. Docking models of the nitrogenase complexes

Docking models were performed using the ClusPro 2.0 protein-protein docking server [39]. Docking models were screened based on salt bridge interactions at the binding interface and with their agreement to the crystal structure of the Mo-nitrogenase complex (PDB entry 4WZB). Models that were a close match were aligned to the Mo-nitrogenase crystal structure to ensure identical conformations between the nitrogenase components before further refinement. The docking models were then uploaded to the HADDOCK 2.2 Water Refinement interface for optimization of residue interactions at the interface [40]. This involves immersing the complex in a solvent shell using the TIP3P water model and running a short 300 K molecular dynamics simulation to allow all side chains to be optimized and improve the energetics of the interaction [40]. All surface electrostatic calculations were carried out using the APBS plugin in PyMOL version 2.2.3 (The PyMOL Molecular

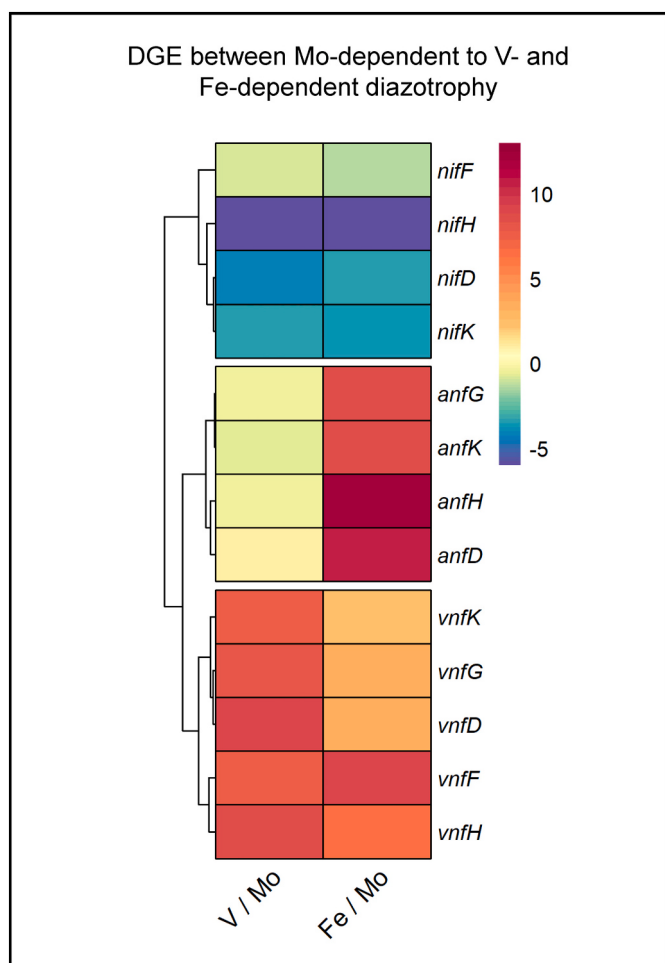


**Fig. 1.** DGE between Mo-dependent and either V- or Fe-dependent diazotrophy. Trends in differential gene expression for the nitrogen-fixation related genes from Mo- to alternative diazotrophy. The heatmap describes the differential gene expression by comparing expression in Mo-dependent growth conditions to that under alternative growth conditions (V/Mo or Fe/Mo).

Graphics System, Schrodinger, LLC).

### 3. Results and discussion

#### 3.1. Differential gene expression between all three nitrogenases

Further analysis of the transcriptomic abundance data expressed as differential gene expression (DGE), enabled patterns to be drawn that explain this tight regulation of the nitrogenase structural genes. The *nif* genes are downregulated 5-fold for both V- and Fe-dependent growth conditions, showing that the lack of Mo leads to repression of the core Mo-nitrogenase structural genes (Fig. 1). V-dependent growth conditions show the upregulation of *vnf* genes only, indicated by a positive fold change in the structural genes for V-nitrogenase (*vnfD*, *vnfK*, *vnfG* and *vnfH*) (Fig. 1). While in Fe-dependent growth conditions, the structural genes for the Fe-nitrogenase (*anfD*, *anfK*, *anfG* and *anfH*) are the most highly upregulated, however genes from the *vnf* gene cluster are also present, mostly as upregulation of *vnfF* and *vnfH* (Fig. 1). The DGE data did show some evidence for crosstalk between the *anf* and *vnf* gene clusters during Fe-dependent growth, which correlates with previous studies that have also implicated crosstalk between the *nif*, *vnf*, and *anf* gene clusters [3,24,25,27–29].

#### 3.2. Modeling the nitrogenase binding interaction

The *in-silico* docking experiments revealed that different surface electrostatics govern the interactions involved in the Fe protein docking to the catalytic component protein in all three nitrogenases (Fig. 2). NifH, VnfH and AnfH share complementary surface electrostatics with its respective catalytic component. NifH and VnfH both show similarly strong negative regions proximal to the [4Fe-4S] cluster and positive regions central to the [4Fe-4S] cluster (Fig. 2A and B). These electrostatic characteristics are complemented on NifDK and VnfDGK, both of which have central negative regions and peripheral positive regions around the P-cluster. The Fe-nitrogenase differs in structural characteristics involved in electron transfer to AnfDGK. The negative regions distal to the [4Fe-4S] cluster of AnfH are much weaker and the central interface around the [4Fe-4S] cluster appears to be more positive (Fig. 2C). The charge differences identified reveal that the pattern of the interactions between AnfH and AnfDGK are different from those in the Mo- or V-nitrogenases and may function to deter cross-reactions between NifH or VnfH with AnfDGK [20,31].

#### 3.3. Residue differences allow for selectivity

Comparing the residues involved in the interactions between NifH, VnfH, AnfH, and their catalytic components reveal that key residue

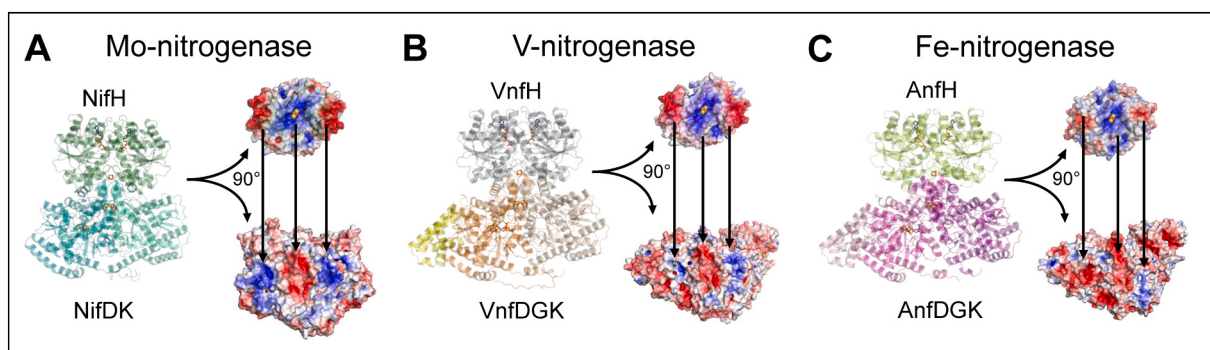


**Fig. 2.** Surface electrostatic potentials for the nitrogenase complexes. A. NifH (green)/NifDK (teal and aqua). B. VnfH (gray)/VnfDGK (orange, yellow, and tan). C. AnfH (light green)/AnfDGK (magenta, pink, purple). Negative charge is shown in red, neutral in white, and positive in blue. For each system, the ribbon structure of the docked complex is shown on the left, and on the right, the Fe protein and its catalytic component are shown rotated 90 degrees to show the surface involved in the docking interaction. (For interpretation of the references to colour in this figure legend, the reader is referred to the web version of this article.)

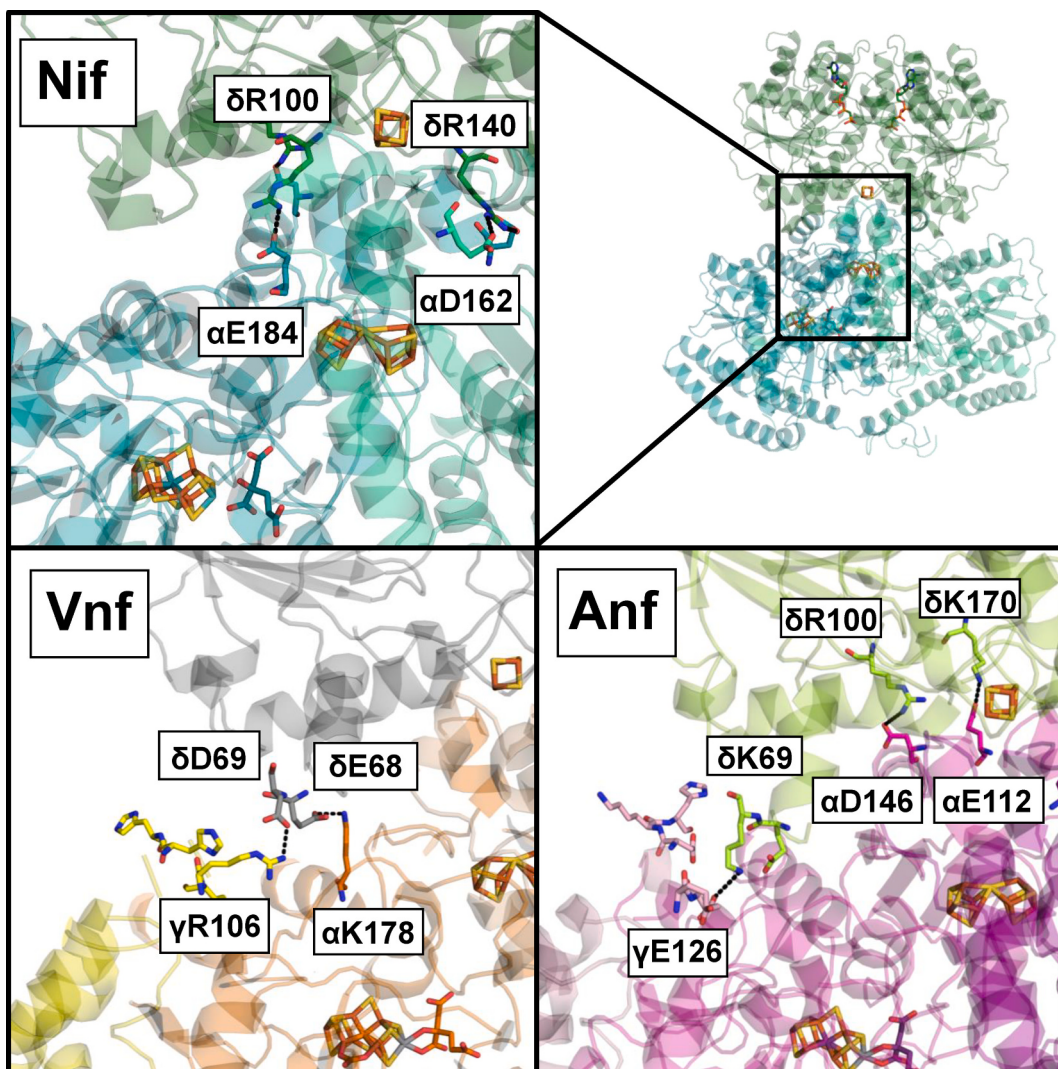


**Fig. 3.** Residue differences at the Fe protein binding site. The three nitrogenases show residue differences that change the electrostatics at the Fe protein binding site. The Mo- (Nif) and V-nitrogenase (Vnf) enzymes have acidic and basic residues on the Fe protein that form salt bridges with acidic and basic residues on NifDK and VnfdDGK: δArg100 and αGlu184 as well as δArg140 of NifH (green) and αAsp162 of NifD (teal). δGlu68 of VnfH (gray) and αLys178 of VnfD (yellow). The Fe-nitrogenase (Anf) uses basic residues on AnfH to form salt bridges to acidic residues on AnfDGK: δArg100 and αAsp146 and δLys170 and αGlu112 of AnfH (light green) and AnfD (magenta). VnfG and AnfG have residues at their C-termini complementary to their Fe proteins: γArg106 of VnfG (yellow) and δAsp69 of VnfH (gray) and γGlu126 of AnfG (pink) and δLys69 of AnfH (light green). (For interpretation of the references to colour in this figure legend, the reader is referred to the web version of this article.)

differences in the Fe proteins are responsible for the observed differences in surface electrostatics. Fig. 3 shows the residues involved in one half of the binding interaction between each Fe protein and the α-subunit or γ-subunit of the corresponding catalytic components.

As shown in Fig. 3, the negative regions at the peripheries of NifH and VnfH can be partially attributed to acidic residues between positions 68 and 69, a region that has previously been implicated as important for nitrogenase complex formation [10,35,41]. AnfH has residue substitutions in this region that explain the positive charge on the binding surface. Amino acid substitutions are shown in the sequence alignment of NifH, VnfH, and AnfH (Fig. S1). Negatively charged glutamic acid residues in NifH and VnfH are exchanged for positively charged lysine at position 69 in AnfH (Fig. S1). Charged residues on the G subunits of VnfdDGK and AnfDGK are shown to form salt bridge interactions with charged residues of their Fe proteins. Positively charged γArg106 on VnfG forms a salt bridge with δAsp69 of VnfH (Fig. 3). Negatively charged γGlu126 of AnfG forms a salt bridge with δLys69 of AnfH (Fig. 3). This implicates a role for the G subunit in binding with its specific Fe protein partner. These differences may function to deter

cross-reactions between NifH or VnfH with AnfDGK.

#### 3.4. Docking studies between VnfdDGK and AnfDGK with NifH, VnfH and AnfH

To test this, VnfdDGK and AnfDGK was docked with NifH, VnfH, and AnfH, and analysis of salt bridge interactions was carried out between AnfG and VnfG and the Fe proteins. The G subunits displayed unique specificity for interactions with its Fe protein component that solely depended on the nature of the charge at the interface. Residues at the C-terminus of the G subunits both interact with residues at position 68 and 69 of the Fe proteins. Sequence alignment of AnfG and VnfG have distinct differences at the interface sites (Fig. S2). Specifically, AnfG has a mixture of positively charged γLys130 and γHis131 residues as well as negatively charged γGlu125, γGlu126 and γAsp129 (Fig. S2). These residues make them extremely complementary to δGlu68 and δLys69 of AnfH. In contrast, VnfG has more positive character at its interface with γArg106 and γHis110 in place of γGlu125 and γAsp129 of AnfG (Fig. S2). γGlu107 and γGlu126 are conserved between the G subunits

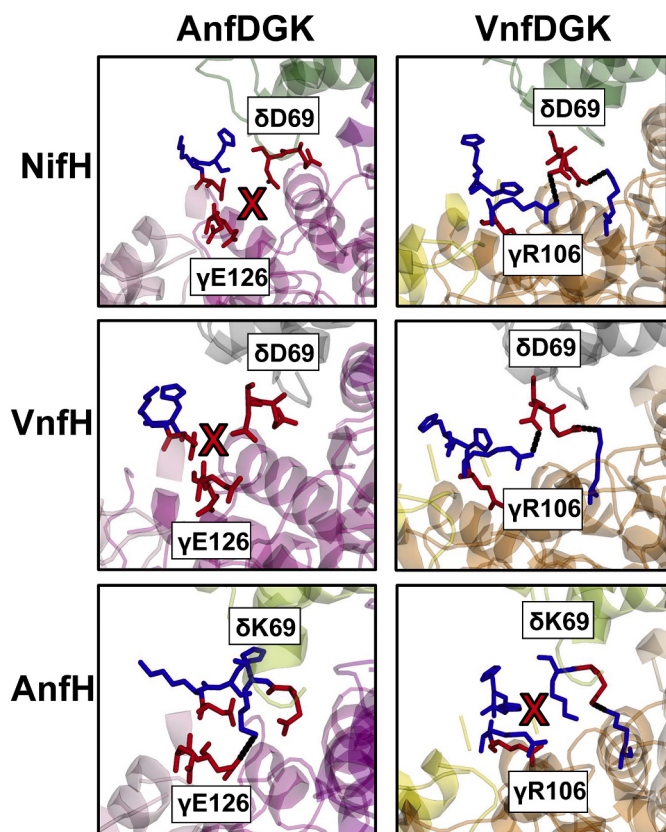


**Fig. 4.** Residue differences between AnfG and VnfG play a role in complementation with the Fe proteins. Left: The negative charge of  $\gamma$ Glu126 (red) on AnfG (pink) repels interactions with negatively charged  $\delta$ Asp69 (red) of VnfH and NifH preventing salt bridge interactions.  $\gamma$ Glu126 (red) of AnfG only forms salt bridges with the positively charged  $\delta$ Lys69 (blue) when docked with AnfH (light green). Right: The positive charge of  $\gamma$ Arg106 (blue) on VnfG (yellow) forms salt bridges with the negatively charged residues,  $\delta$ Asp69 (red), when docked with NifH and VnfH.  $\gamma$ Arg106 (blue) of VnfG is repelled by the positive charge of  $\delta$ Lys69 (blue) preventing salt bridge interactions when docked with AnfH. (For interpretation of the references to colour in this figure legend, the reader is referred to the web version of this article.)

(Fig. S2). This more positively charged interface for VnfG makes it complementary for interactions with  $\delta$ Glu68 and  $\delta$ Asp69 of VnfH and NifH.

Indeed, salt bridge interactions were not observed between any of the residues on AnfG and NifH or VnfH (Fig. 4). The negative charge of Glu68 and Asp69 repelled interactions because of the negative charge of  $\gamma$ Glu125 and  $\gamma$ Glu126 on AnfG (Fig. 4, left). In contrast, salt bridge interactions were observed between  $\gamma$ Arg106 of VnfG and  $\delta$ Asp69 for both NifH and VnfH (Fig. 4, right). No salt bridge interactions were observed for  $\gamma$ Arg106 of VnfG and  $\delta$ Glu68 as a result of the interference by  $\delta$ Lys69 of AnfH at that position (Fig. 4, right). This implies that the G subunit could play a role in selectivity of VnfDGK and AnfDGK for their Fe protein components. Furthermore, it was observed in the crystal structure of VnfDGK that the G subunit is positioned to not interfere with complex formation [20]. The salt bridges identified in our docking model indicate that the G subunit does not interfere, but could in fact aid in complex formation between VnfDGK and VnfH as well as AnfDGK and AnfH.

#### 4. Conclusions

Ultimately, the protein-protein docking results combined with the DGE analysis build a rich picture for regulating electron transfer between the three nitrogenase enzymes. The models of each nitrogenase

show that surface electrostatics plays a major role in complex formation and that the Fe-nitrogenase shows unique surface electrostatics compared to the Mo- and V-nitrogenases. The Fe proteins also show complementary electrostatics to their catalytic components and AnfH has key residue differences compared to NifH and VnfH at position 69 that have a major effect on interactions with its docking partners. This is especially true for VnfDGK and AnfDGK, where the G subunit seems to play a role in recognition of its complementary Fe protein partner.

The differences in the electrostatics that govern nitrogenase interactions would be expected to reduce the number of efficient electron transfer events that lead to the Fe-nitrogenase. The high metabolic cost for nitrogen fixation coupled with the diversity of soil environments where *A. vinelandii* resides, implicates that *A. vinelandii* would need to adapt expression of each nitrogenase in coordination with metal availability in its environment. The G subunit has been co-opted to provide a mechanism that could allow *A. vinelandii* to express the alternative nitrogenases under Mo-limited conditions while still enabling the use of the Mo-nitrogenase to fix  $N_2$ . For example, in environmental conditions where there are higher amounts of V compared to Mo, VnfH could be redirected to support nitrogen fixation by NifDK over VnfDGK.

This is supported by the modeling data, where charge differences were defined at the G subunit that serve to increase the number of possible pathways of electron delivery to the Mo-nitrogenase, effectively funneling electrons to the most efficient enzyme. This provides a mechanism to explain the biochemical data that show crosstalk between the Mo- and V-nitrogenase components but not the Fe-nitrogenase. Structurally differentiating the Fe-nitrogenase in this way would reduce competition between the Mo- and Fe-nitrogenases, leaving NifH and VnfH free to associate with NifDK.

#### Declaration of Competing Interest

The authors declare that they have no conflicts of interest with the contents of this article.

#### Acknowledgement

This work was supported as part of the Biological Electron Transfer and Catalysis Energy Frontier Research Center funded by the U.S. Department of Energy, Office of Science, Basic Energy Sciences under Award # DE-SC0019447.

#### Appendix A. Supplementary data

Supplementary data to this article can be found online at <https://doi.org/10.1016/j.jinorgbio.2020.111273>.

#### References

- [1] Y. Hu, M.W. Ribbe, Nitrogenase and homologs, *J. Biol. Inorg. Chem.* 20 (2015) 435–445, <https://doi.org/10.1007/s00775-014-1225-3>.
- [2] B.M. Hoffman, D. Lukyanov, Z.Y. Yang, D.R. Dean, L.C. Seefeldt, Mechanism of nitrogen fixation by nitrogenase: the next stage, *Chem. Rev.* 114 (2014) 4041–4062, <https://doi.org/10.1021/cr400641x>.
- [3] R.R. Eady, Structure-function relationships of alternative nitrogenases, *Chem. Rev.* 96 (1996) 3013–3030, <https://doi.org/10.1021/cr950057h>.
- [4] R.N. Thorneley, D.J. Lowe, The mechanism of *Klebsiella pneumoniae* nitrogenase action. Pre-steady-state kinetics of an enzyme-bound intermediate in  $N_2$  reduction and of  $NH_3$  formation, *Biochem. J.* 224 (1984) 887–894, <https://doi.org/10.1042/bj2240887>.
- [5] R.V. Hageman, R.H. Burris, Nitrogenase and nitrogenase reductase associate and dissociate with each catalytic cycle, *Proc. Natl. Acad. Sci. U. S. A.* 75 (1978) 2699–2702, <https://doi.org/10.1073/pnas.75.6.2699>.
- [6] M.K. Chan, J. Kim, D.C. Rees, The nitrogenase FeMo-cofactor and P-cluster pair: 2.2 Å resolution structures, *Science* 260 (1993) 792–794, <https://doi.org/10.1126/science.8484118>.
- [7] K.M. Lancaster, M. Roemelt, P. Ettenhuber, Y. Hu, M.W. Ribbe, F. Neese, U. Bergmann, S. DeBeer, X-ray emission spectroscopy evidences a central carbon in the nitrogenase iron-molybdenum cofactor, *Science* 334 (2011) 974–977, <https://doi.org/10.1126/science.1206445>.

- [8] M.M. Georgiadis, H. Komiya, P. Chakrabarti, D. Woo, J.J. Kornuc, D.C. Rees, Crystallographic structure of the nitrogenase iron protein from *Azotobacter vinelandii*, *Science* 257 (1992) 1653–1659, <https://doi.org/10.1126/science.1529353>.
- [9] Z.Y. Yang, R. Ledbetter, S. Shaw, N. Pence, M. Tokmina-Lukaszewska, B. Eilers, Q. Guo, N. Pokhrel, V.L. Cash, D.R. Dean, E. Antony, B. Bothner, J.W. Peters, L. C. Seefeldt, Evidence that the P<sub>i</sub> release event is the rate-limiting step in the nitrogenase catalytic cycle, *Biochemistry* 55 (2016) 3625–3635, <https://doi.org/10.1021/acs.biochem.6b00421>.
- [10] N. Pence, M. Tokmina-Lukaszewska, Z.Y. Yang, R.N. Ledbetter, L.C. Seefeldt, B. Bothner, J.W. Peters, Unraveling the interactions of the physiological reductant flavodoxin with the different conformations of the Fe protein in the nitrogenase cycle, *J. Biol. Chem.* 292 (2017) 15661–15669, <https://doi.org/10.1074/jbc.M117.801548>.
- [11] S. Duval, K. Danyal, S. Shaw, A.K. Lytle, D.R. Dean, B.M. Hoffman, E. Antony, L. C. Seefeldt, Electron transfer precedes ATP hydrolysis during nitrogenase catalysis, *Proc. Natl. Acad. Sci. U. S. A.* 110 (2013) 16414–16419, <https://doi.org/10.1073/pnas.1311218110>.
- [12] K. Danyal, D.R. Dean, B.M. Hoffman, L.C. Seefeldt, Electron transfer within nitrogenase: evidence for a deficit-spending mechanism, *Biochemistry* 50 (2011) 9255–9263, <https://doi.org/10.1021/bi201003a>.
- [13] K. Danyal, D. Mayweather, D.R. Dean, L.C. Seefeldt, B.M. Hoffman, Conformational gating of electron transfer from the nitrogenase Fe protein to MoFe protein, *J. Am. Chem. Soc.* 132 (2010) 6894–6895, <https://doi.org/10.1021/ja101737f>.
- [14] L.C. Seefeldt, B.M. Hoffman, J.W. Peters, S. Raugei, D.N. Beratan, E. Antony, D. R. Dean, Energy transduction in nitrogenase, *Acc. Chem. Res.* 51 (2018) 2179–2186, <https://doi.org/10.1021/acs.accounts.8b00112>.
- [15] R.N. Thorneley, D.J. Lowe, Nitrogenase of *Klebsiella pneumoniae*. Kinetics of the dissociation of oxidized iron protein from molybdenum-iron protein: identification of the rate-limiting step for substrate reduction, *Biochem. J.* 215 (1983) 393–403, <https://doi.org/10.1042/bj2150393>.
- [16] D.F. Harris, D.A. Lukyanov, H. Kallas, C. Trncik, Z.Y. Yang, P. Compton, N. Kelleher, O. Einsle, D.R. Dean, B.M. Hoffman, L.C. Seefeldt, Mo-, V-, and Fe-nitrogenases use a universal eight-electron reductive-elimination mechanism to achieve N<sub>2</sub> reduction, *Biochemistry* 58 (2019) 3293–3301, <https://doi.org/10.1021/acs.biochem.9b00468>.
- [17] F. Simpson, R.H. Burris, A nitrogen pressure of 50 atmospheres does not prevent evolution of hydrogen by nitrogenase, *Science* 224 (1984) 1095–1097, <https://doi.org/10.1126/science.6585956>.
- [18] F. Mus, A.B. Alleman, N. Pence, L.C. Seefeldt, J.W. Peters, Exploring the alternatives of biological nitrogen fixation, *Metalomics* 10 (2018) 523–538, <https://doi.org/10.1039/c8mt00038g>.
- [19] K. Schneider, U. Gollan, M. Drötsboom, S. Selsemeier-Voigt, A. Müller, Comparative biochemical characterization of the iron-only nitrogenase and the molybdenum nitrogenase from *Rhodobacter capsulatus*, *Eur. J. Biochem.* 244 (1997) 789–800, <https://doi.org/10.1111/j.1432-1033.1997.t01-1-00789.x>.
- [20] D. Sippel, O. Einsle, The structure of vanadium nitrogenase reveals an unusual bridging ligand, *Nat. Chem. Biol.* 13 (2017) 956–960, <https://doi.org/10.1038/ncbimio.2428>.
- [21] S.I. Waugh, D.M. Paulsen, P.V. Mylona, R.H. Maynard, R. Premakumar, P. E. Bishop, The genes encoding the delta subunits of dinitrogenases 2 and 3 are required for Mo-independent diazotrophic growth by *Azotobacter vinelandii*, *J. Bacteriol.* 177 (1995) 1505–1510, <https://doi.org/10.1128/jb.177.6.1505-1510.1995>.
- [22] R. Chatterjee, P.W. Ludden, V. Shah, Characterization of VNFG, the δ Subunit of the vnf-Encoded Apodinitrogenase from *Azotobacter vinelandii*, *J. Biol. Chem.* 272 (1997) 3758–3765, <https://doi.org/10.1074/jbc.272.6.3758>.
- [23] E. Krahn, B.J.R. Weiss, M. Kröckel, J. Groppe, G. Henkel, S.P. Cramer, A. X. Trautwein, K. Schneider, A. Müller, The Fe-only nitrogenase from *Rhodobacter capsulatus*: identification of the cofactor, an unusual, high-nuclearity iron-sulfur cluster, by Fe K-edge EXAFS and 57Fe Mössbauer spectroscopy, *J. Biol. Inorg. Chem.* 7 (2002) 37–45, <https://doi.org/10.1007/s00750100263>.
- [24] R.R. Eady, R.L. Robson, T.H. Richardson, R.W. Miller, M. Hawkins, The vanadium nitrogenase of *Azotobacter chroococcum*. Purification and properties of the VFe protein, *Biochem. J.* 244 (1987) 197–207, <https://doi.org/10.1042/bj2440197>.
- [25] T.L. Hamilton, M. Ludwig, R. Dixon, E.S. Boyd, P.C. Dos Santos, J.C. Setubal, D. A. Bryant, D.R. Dean, J.W. Peters, Transcriptional profiling of nitrogen fixation in *Azotobacter vinelandii*, *J. Bacteriol.* 193 (2011) 4477–4486, <https://doi.org/10.1128/JB.05099-11>.
- [26] J.C. Setubal, P. Dos Santos, B.S. Goldman, H. Ertesvåg, G. Espin, L.M. Rubio, S. Valla, N.F. Almeida, D. Balasubramanian, L. Cromes, L. Curatti, Z. Du, E. Godsy, B. Goodner, K. Hellner-Burris, J.A. Hernandez, K. Houmiel, J. Imperial, C. Kennedy, T.J. Larson, P. Latreille, L.S. Ligon, J. Lu, M. Mærk, N.M. Miller, S. Norton, I.P. O'Carroll, I. Paulsen, E.C. Raulfs, R. Roemer, J. Rosser, D. Segura, S. Slater, S.L. Stricklin, D.J. Studholme, J. Sun, C.J. Viana, E. Wallin, B. Wang, C. Wheeler, H. Zhu, D.R. Dean, R. Dixon, D. Wood, Genome sequence of *Azotobacter vinelandii*, an obligate aerobe specialized to support diverse anaerobic metabolic processes, *J. Bacteriol.* 191 (2009) 4534–4545, <https://doi.org/10.1128/JB.00504-09>.
- [27] R.D. Joerger, M.R. Jacobson, R. Premakumar, E.D. Wolfinger, P.E. Bishop, Nucleotide sequence and mutational analysis of the structural genes (*anfHDGK*) for the second alternative nitrogenase from *Azotobacter vinelandii*, *J. Bacteriol.* 171 (1989) 1075–1086, <https://doi.org/10.1128/jb.171.2.1075-1086.1989>.
- [28] R.D. Joerger, T.M. Loveless, R.N. Pau, L.A. Mitchenall, B.H. Simon, P.E. Bishop, Nucleotide sequences and mutational analysis of the structural genes for nitrogenase 2 of *Azotobacter vinelandii*, *J. Bacteriol.* 172 (1990) 3400–3408, <https://doi.org/10.1128/jb.172.6.3400-3408.1990>.
- [29] R.D. Joerger, R. Premakumar, P.E. Bishop, Tn5-induced mutants of *Azotobacter vinelandii* affected in nitrogen fixation under Mo-deficient and Mo-sufficient conditions, *J. Bacteriol.* 168 (1986) 673–682, <https://doi.org/10.1128/jb.168.2.673-682.1986>.
- [30] C. Kennedy, P. Rudnick, T. MacDonald, T. Melton, Azotobacter, in: G.M. Garrity (Ed.), *Bergey's manual of systematic bacteriology*, Springer, New York, New York, 2005, pp. 384–401.
- [31] D. Sippel, J. Schlesier, M. Rohde, C. Trncik, L. Decamps, I. Djurdjevic, T. Spatzl, S. L.A. Andrade, O. Einsle, Production and isolation of vanadium nitrogenase from *Azotobacter vinelandii* by molybdenum depletion, *J. Biol. Inorg. Chem.* 22 (2017) 161–168, <https://doi.org/10.1007/s00775-016-1423-2>.
- [32] B.S. Pratte, K. Eplin, T. Thiel, Cross-functionality of nitrogenase components NifH1 and VnfH in *Anabaena variabilis*, *J. Bacteriol.* 188 (2006) 5806–5811, <https://doi.org/10.1128/JB.00618-06>.
- [33] O. Einsle, F.A. Tezcan, S.L.A. Andrade, B. Schmid, M. Yoshida, J.B. Howard, D. C. Rees, Nitrogenase MoFe-protein at 1.16 Å resolution: a central ligand in the FeMo-cofactor, *Science* 297 (2002) 1696–1700, <https://doi.org/10.1126/science.1073877>.
- [34] C.P. Owens, F.E.H. Katz, C.H. Carter, M.A. Luca, F.A. Tezcan, Evidence for functionally relevant encounter complexes in nitrogenase catalysis, *J. Am. Chem. Soc.* 137 (2015) 12704–12712, <https://doi.org/10.1021/jacs.5b08310>.
- [35] F.A. Tezcan, J.T. Kaiser, D. Mustafi, M.Y. Walton, J.B. Howard, D.C. Rees, Nitrogenase complexes: multiple docking sites for a nucleotide switch protein, *Science* 309 (2005) 1377–1381, <https://doi.org/10.1126/science.1115653>.
- [36] M. Rohde, C. Trncik, D. Sippel, S. Gerhardt, O. Einsle, Crystal structure of VnfH, the iron protein component of vanadium nitrogenase, *J. Biol. Inorg. Chem.* 23 (2018) 1049–1056, <https://doi.org/10.1007/s00775-018-1602-4>.
- [37] G.R. Warnes, B. Bolker, L. Bonebakker, R. Gentleman, W. Huber, A. Liaw, T. Lumley, M. Maechler, A. Magnusson, S. Moeller, M. Schwartz, gplots: Various R programming tools for plotting data, in: R Package Version 2(4), 2009, p. 1.
- [38] A. Waterhouse, M. Bertoni, S. Bienert, G. Studer, G. Tauriello, R. Gumienny, F. T. Heer, T.A.P. De Beer, C. Rempfer, L. Bordoli, R. Lepore, T. Schwede, SWISS-MODEL: homology modeling of protein structures and complexes, *Nucleic Acids Res.* 46 (2018) W296–W303, <https://doi.org/10.1093/nar/gky427>.
- [39] D. Kozakov, D.R. Hall, B. Xia, K.A. Porter, D. Padhorney, C. Yueh, D. Beglov, S. Vajda, The ClusPro web server for protein-protein docking, *Nat. Protoc.* 12 (2017) 255–278, <https://doi.org/10.1038/nprot.2016.169>.
- [40] G.C.P. Van Zundert, J.P.G.L.M. Rodrigues, M. Trellet, C. Schmitz, P.L. Kastritis, E. Karaca, A.S.J. Melquiond, M. Van Dijk, S.J. De Vries, A.M.J.J. Bonvin, M. Sternberg, The HADDOCK2.2 web server: user-friendly integrative modeling of biomolecular complexes, *J. Mol. Biol.* 428 (2016) 720–725, <https://doi.org/10.1016/j.jmb.2015.09.014>.
- [41] J.W. Peters, K. Fisher, D.R. Dean, Identification of a nitrogenase protein-protein interaction site defined by residues 59 through 67 within *Azotobacter vinelandii*, *J. Biol. Chem.* 269 (1994) 28076–28083.